Inorg. Chem. **2005**, *44*, 1983–1991

Theoretical and Synthetic Investigations of Carbodiimide Insertions into Al–CH_3 and Al–$N(CH_3)_2$ Bonds

Christopher N. Rowley,[†] Gino A. DiLabio,*[,‡] and Seán T. Barry*[,†]

Department of Chemistry, Carleton University, Ottawa, 1125 Colonel By Drive, Ontario, Canada K1S 5B6, and National Institute for Nanotechnology, National Research Council of Canada, W6-010 ECERF, 9107-116th Street, Edmonton, Alta., Canada T6G 2V4

Received October 26, 2004

Carbodiimides are known to insert into aluminum–carbon bonds to form four-membered bidentate amidinate chelate rings. Insertions into Al–R and Al–NR'_2 (R, R′ = alkyl) have been reported in the literature. We have devised a mechanism for these insertions and modeled it using density functional theory (DFT) calculations. The calculated barrier heights for competitive insertions show the insertion into Al–$N(CH_3)_2$ goes through a lower barrier than the reaction with Al–CH_3 for diisopropyl carbodiimide due to the necessity of forming a pentavalent carbon intermediate in the Al–CH_3 case. However, insertion into Al–CH_3 has the lower barrier for the reaction with di-*tert*-butyl carbodiimide because of steric effects, which is consistent with the published experimental results. We have synthesized aluminum amidinates containing two and three acetamidinate rings via insertion of 2 and 3 equiv of diisopropylcarbodiimide into trimethylaluminum (TMA). The crystal structure for $[CH_3C(N^iPr)_2]_2AlCH_3$ is reported. We have found that, although the first insertion is rapid at room temperature, the second and third insertions require refluxing above 70 °C. We have calculated the barrier heights for the first and second insertion and have found that this is due to a higher barrier for the migration of the methyl group in the second insertion. This higher barrier is the result of the lack of an exergic precoordination of the carbodiimide to the metal center, which facilitates the first insertion.

Introduction

Amidinates have been long studied as chelating ligands for main group, transition metal, and f-block elements.[1] Aluminum amidinates are of interest as potential reagents in organic synthesis,[2] as catalysts for olefin polymerization,[3] and as precursors for thin film deposition.[4] One method for synthesizing amidinates is the reaction of M−R (where R = H, or alkyl) with a carbodiimide (R′−N═C═N−R′; R′ = alkyl). The carbodiimide can insert into one of the bonds to the metal center to form a four-membered ring wherein the two nitrogens of the carbodiimide are coordinated to the metal center and the R group originally bonded to the metal center has migrated to the sp carbon of the carbodiimide,

Scheme 1

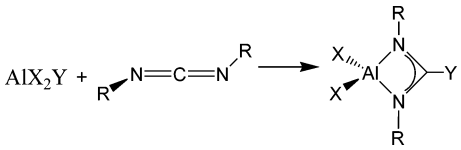

causing it to adopt sp^2 hybridization (Scheme 1). The use of carbodiimide insertions for the synthesis of amidinates has the advantage of being facile and typically results in high yields.[5−7] Furthermore, for the particular application of thin film precursor synthesis, carbodiimide insertions avoid salt metathesis reactions that are frequently employed in aluminum amidinate synthesis, thereby preventing halogen impurities in the target films, which can impair the electrical properties of the deposited film.

Carbodiimide insertions fall into the larger class of heterocumulene insertions. Other heterocumulenes, such as carbon dioxide and isothiocyanates, can undergo analogous

* Authors to whom correspondence should be addressed. E-mail: sbarry@ccs.carleton.ca (S.T.B.); gino.dilabio@nrc-cnrc.gc.ca (G.A.D.).
† Carleton University.
‡ National Research Council of Canada.

(1) Barker, J.; Kilner, M. *Coord. Chem. Rev.* **1994**, *133*, 219.
(2) Chang, C.-C.; Chen, J.-H.; Srinivas, B.; Chiang, M. Y.; Lee, G.-H. *Organometallics* **1997**, *16*, 4980.
(3) Coles, M. P.; Swenson, D. C.; Jordan, R. F.; Young, V. G., Jr. *Organometallics* **1997**, *16*, 5183.
(4) Lim, B. S.; Rahtu, A.; Park, J.-S.; Gordon, R. G. *Inorg. Chem.* **2003**, *42*, 7951.
(5) Chang, C.-C.; Hsiung, C.-S.; Su, H.-L.; Srinivas, B.; Chiang, M. Y.; Lee, G.-H.; Wang, Y. *Organometallics* **1998**, *17*, 1595.
(6) Coles, M. P.; Hitchcock, P. B. *Eur. J. Inorg. Chem.* **2004**, 2662.
(7) Kenney, A. P.; Richeson, D.; Barry, S. T., unpublished results.

10.1021/ic048501z CCC: $30.25
Published on Web 02/08/2005

insertion reactions. Carbon dioxide insertions are of particular interest due to their potential as a CO_2 fixation reaction. For this reason, Gambarotta and co-workers studied the mechanism of insertion of several heterocumulenes into zirconium−alkyl bonds.[8] For the particular case of carbodiimide insertions, they proposed that the coordination of one of the nitrogen atoms of the carbodiimide to the acid metal center promotes the polarization of the N═C═N segment, facilitating the migration of the alkyl group. This precoordination also places the alkyl group and the inserting molecule into close proximity, which aids insertion.

Tunge et al. came to similar conclusions based on their own investigations of carbodiimide insertions into zirconium−alkyl bonds in zirconaaziridines with THF present as a dative base.[9] They observed that the rate of insertion was inversely proportional to the concentration of THF, indicating that the THF ligand must dissociate before the carbodiimide insertion. They concluded that it is necessary for carbodiimide to coordinate to the metal center for the insertion to occur.

Although there has been a considerable amount of experimental investigation into carbodiimide insertions, little theoretical work has been done. The mechanism of ethylene polymerization has previously been modeled using DFT calculations.[10] The analogous insertion of carbon dioxide insertion into a rhodium(III)−hydride bond has been investigated using computational methods by Musashi and Sakaki.[11] In this reaction, carbon dioxide inserts into the Rh−H bond to generate a formate ligand. The mechanism proposed in their study was a three-step process: (i) one oxygen atom of the carbon dioxide coordinates to the metal center, forming a dative bond; (ii) the hydrogen bonded to the rhodium center migrates to the sp carbon of the carbon dioxide; and (iii) the second oxygen of the carbon dioxide coordinates to the metal center, forming the product. These researchers found that the insertion process has two separate transition states, as there is a metastable intermediate formed after the hydrogen migrates but before the second oxygen coordinates. As the first barrier was much larger than the second, they concluded that the first reaction step was rate determining.

Carbodiimide insertions into aluminum alkyl and amino bonds have not been explored this thoroughly. Chang and co-workers have done the most extensive work on the mechanism of these particular reactions.[5] They determined experimentally that when an aluminum center contained both Al−R and Al−NR′$_2$ bonds, diisopropyl carbodiimide would preferentially insert into the Al−NR′$_2$ bond (R, R′ = alkyl). Conversely, di-*tert*-butyl-carbodiimide would preferentially insert into the Al−R bond (Scheme 2).

Pioneering work by Dehnicke showed insertion of bis(trimethylsilyl)carbodiimide into an aluminum aryl bond,[12] and Weidlein and co-workers reported a facile insertion of

Scheme 2

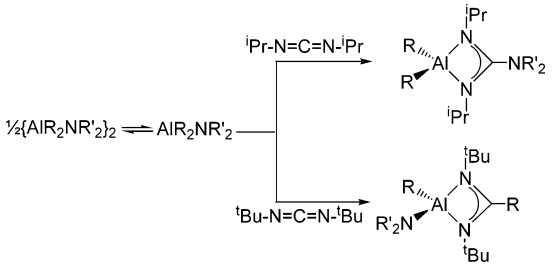

the same carbodiimide into trimethyl aluminum to form the monomeric insertion product at room temperature.[13] Jordan and co-workers subsequently synthesized a four-coordinate aluminum acetamidinate via the insertion of diisopropyl carbodiimide into trimethylaluminum (TMA), although they did not report products for the analogous second and third insertions.[3] The five- and six-coordinate acetamidinates may have utility as precursors for thin film deposition, so we are interested in developing these syntheses. In a previous study, we have synthesized five- and six-coordinate guanidinates by inserting multiple carbodiimides into homoleptic aluminum amide,[7] demonstrating that it is possible to synthesize five- and six-coordinate aluminum amidinates by carbodiimide insertion. This indicates that it may be possible to synthesize analogous acetamidinates by multiple carbodiimide insertion into a trimethylaluminum.

Clearly, elucidating a reaction mechanism for carbodiimide insertion into aluminum alkyl and amino bonds would improve our understanding of these reactions. Determining the importance of the coordination of the carbodiimide in these reactions will help clarify whether it is essential for a carbodiimide to coordinate to the metal center before insertion, as has been suggested by work done on other systems. To better understand the role of precoordination, the insertion preference order reported by Chang and co-workers, and the results of our own synthesis, we have undertaken a mechanistic study of these systems using density functional theory (DFT) calculations.

Results and Discussion

Reaction Mechanism. Our preliminary computations found that a mechanism analogous to the one proposed by Musashi and Sakaki was also valid for carbodiimide insertions into three-coordinate aluminum centers. The key difference in the case of carbodiimides is that the intermediate structures for carbodiimide insertions are considerably more stable and the second barrier for the chelation of the amidinate ligand is much higher than the barrier for the second transition state of the carbon dioxide insertion. On the basis of these results, we outlined a mechanism that we have applied throughout this work (Scheme 3):

(1) A lone-pair of one of the nitrogen atoms of the carbodiimide coordinates via a dative bond to the aluminum center, forming an adduct.

(2) One of the aluminum center's ligands migrates from the metal to the sp-hybridized carbon of the carbodiimide, forming a reaction intermediate (TS1).

(8) Gambarotta, S.; Strologo, S.; Floriani, C.; Chiesi-Villa, A.; Guastini, C. *Inorg. Chem.* **1985**, *24*, 654.
(9) Tunge, J. A.; Czerwinski, C. J.; Gately, D. A.; Norton, J. R. *Organometallics* **2001**, *20*, 254.
(10) Talarico, G.; Budzelaar, P. H. M. *Organometallics* **2000**, *19*, 5691.
(11) Musashi, Y.; Sakaki, S. *J. Chem. Soc., Dalton Trans.* **1998**, 577.
(12) Ergezinger, C.; Weller, F.; Dehnicke, K. *Z. Naturforsch.* **1988**, *43b*, 1621.
(13) Lechler, R.; Hausen, H. D.; Weidlein, J. *J. Organomet. Chem.* **1989**, *359*, 1.

Scheme 3. The Proposed Mechanism for Carbodiimide Insertion

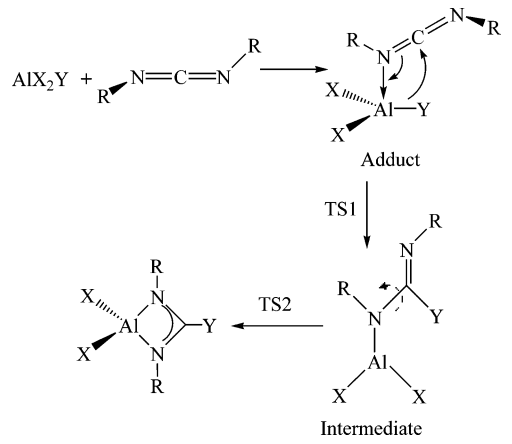

Table 1. Relative Energies of Diisopropyl and Di-*tert*-butyl Carbodiimide Insertion into H_2Al-Y Bonds[a]

R	Y	separated	adduct	TS1	intermediate	TS2	product
^{i}Pr	$N(CH_3)_2$	0.0	−17.1	−8.4	−26.6	−1.3	−36.1
	CH_3	0.0	−21.4	4.9	−29.2	−24.4	−59.6
^{t}Bu	$N(CH_3)_2$	0.0	−14.9	−4.3	−15.2	12.0	−23.1
	CH_3	0.0	−16.7	9.2	−18.2	−14.6	−47.2

[a] All values are calculated using BH&HLYP/6-311g(2d,2p)//BH&HLYP/6-31g(d) and are reported in kcal mol^{-1}.

(3) The second nitrogen of the carbodiimide coordinates to the metal center to form the product (TS2).

The insertion preference of carbodiimides reported by Chang is a useful test of the validity of the reaction mechanism proposed here. Reaction energies and barrier heights for the insertion of diisopropyl and di-*tert*-butyl carbodiimides were calculated for insertion into H_2Al-CH_3 and $H_2Al-N(CH_3)_2$ bonds. These compounds are used to model alkyl and dialkyl amino ligands to determine if calculations following this mechanism correctly predict the insertion preference. The energetic results are summarized in Table 1. The reaction profiles are plotted in Figure 1a,b, and schematics of the stationary points and key bond lengths are reported in Figure 2.

Coordination. The coordination energies of the carbodiimide to the three-coordinate aluminum center vary with both the carbodiimide being inserted and the substituents on the aluminum center. For both carbodiimides, the adduct with H_2Al-CH_3 is more stable than it is with $H_2Al-N(CH_3)_2$ due to the greater degree of electron donation by the amino group, which decreases the electrophilicity of the aluminum center. For both migrating groups, the isopropyl carbodiimide adducts are more stable than the adducts with the *tert*-butyl groups, due to the larger degree of steric repulsion between the di-*tert*-butyl carbodiimide and the aluminum compound. In each case, the ligands of the aluminum center are pushed slightly out of a planar arrangement. For all systems studied, there is a stable conformation wherein the carbodiimide eclipses the bond of insertion. This arrangement minimizes the repulsion between the R′ group bonded to the nitrogen coordinated to the metal center and the other ligands of the aluminum center. This adduct puts the reactants into a suitable geometrical conformation for a group on the aluminum center to migrate to the sp carbon of the carbodiimide. In each case, the formation of the adduct is significantly exergic, ranging from −14.9 to −23.4 kcal mol^{-1}. This step serves to stabilize all subsequent points on the reaction coordinate, effectively lowering the barrier heights for the insertion.

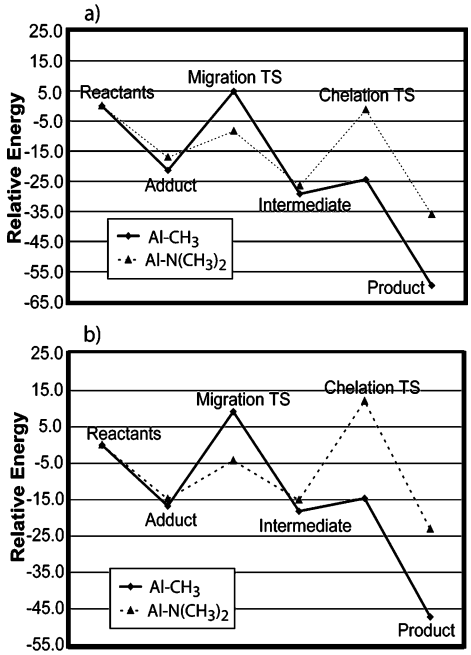

Figure 1. BH&HLYP/6-311g(2d,2p)/BH&HLYP/6-31g(d) gas-phase energy profile for the insertion of diisopropyl carbodiimide (a) and di-*tert*-butyl-carbodiimide (b) into H_2Al-CH_3 and $H_2Al-N(CH_3)_2$ bonds. All values are in kcal mol^{-1}.

Migration. In the first transition state, the group migrating from the aluminum center bends out of plane toward the sp carbon of the carbodiimide. This step involves a significant shortening in the bond length of the coordinated nitrogen of the carbodiimide and the aluminum center, indicating a change from a dative bond into a covalent bond. This contraction brings the p-orbitals involved in the carbodiimide π-system into bonding range of the migrating group. At the transition state, the alkyl group bonded to the exocyclic nitrogen of the carbodiimide rotates from its near-orthogonal position toward a position in-plane with the aluminum center. Also, the N=C=N segment of the carbodiimide becomes more asymmetrical, with a larger bend in the ∠NCN angle, indicating that the carbodiimide undergoes a considerable electronic rearrangement before the transition state is reached.

The height of the migration barrier depends heavily on the group that migrates. The transition state has a relative energy of −8.4 kcal mol^{-1} for the amino insertion but 4.9 kcal for the methyl insertion. This difference can be attributed to the lone-pair on the nitrogen of the dimethyl amino moiety. At the migration transition state, the dimethyl amino group adopts a tetrahedral geometry with its lone-pair directed toward the sp-hybridized carbon, which facilities the formation of the C−N bond. The methyl insertion goes though a more typical transition state, where the methyl group adopts a pentavalent geometry and the bonds involved in the reaction are substantially stretched from their equilibrium positions. There is no contribution by other bonding modes as in the

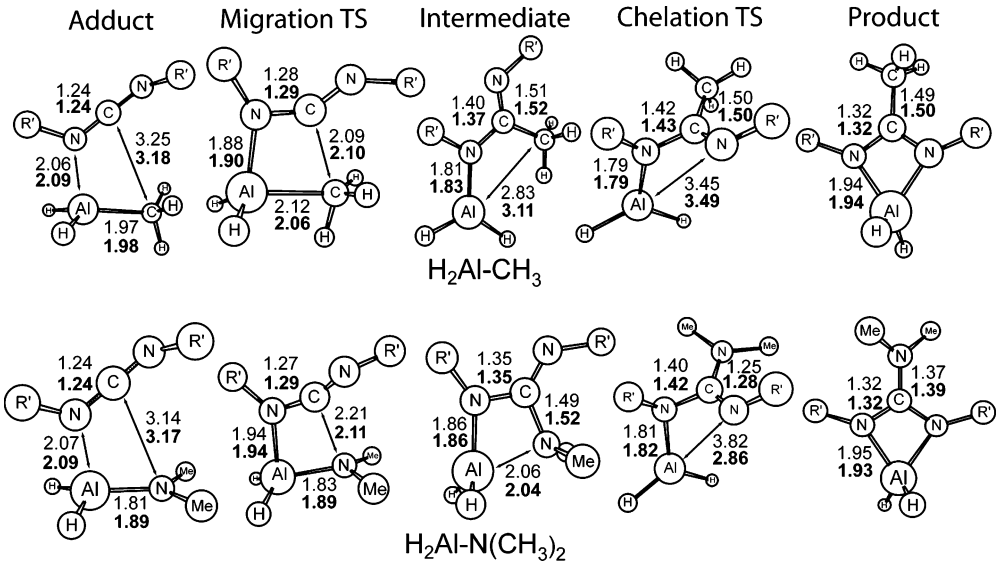

Figure 2. Schematics of the stationary points for the insertion of carbodiimide into H_2Al-CH_3 (top) and $H_2Al-N(CH_3)_2$ (bottom) (R′ = ^{i}Pr, ^{t}Bu). Key bond lengths are included adjacent to the bonds. Values for ^{i}Pr carbodiimide are in regular type and are the topmost set of numbers. Values for ^{t}Bu carbodiimide are in bold type and are the bottommost set of numbers.

dimethyl amino insertion case. On the basis of these differences, it can be generally stated that alkyl groups make relatively poor groups for migration in these insertions due the highly distorted geometry that the group has to adopt to migrate.

The substitution of di-*tert*-butyl carbodiimide for diisopropyl carbodiimide has a fairly constant effect on the migration barriers. The barrier heights for the *tert*-butyl insertions are 4.1 kcal mol^{-1} higher than the isopropyl insertion for the dimethyl amino insertion, and 4.3 kcal mol^{-1} higher for methyl insertion. This increase is due to the greater steric repulsion between the R′ group and the migrating group.

Intermediate. After the migration step, a metastable intermediate is formed. The bond between the nitrogen of the carbodiimide and the aluminum center shortens from a typical dative bond length to a typical covalent bond length. In the dimethyl amino insertions, the lone-pair of the amino group remains coordinated to the aluminum center, although at a dative rather than covalent bond length. In contrast, the H_2Al-CH_3 insertion intermediate forms a nearly planar arrangement where the aluminum is in plane with the singly coordinated amidinate ligand. This planar arrangement allows the N−C═N π-system of the amidinate ligand to conjugate with the empty p-orbital of the aluminum center.

Chelation Transition State. To form the product, the intermediate must rotate around the C−N bond so that the second nitrogen of the amidinate can coordinate to the aluminum center. This barrier is higher than for a typical rotation around a σ-bond due to conjugation between the lone-pair of the coordinated nitrogen and the sp^2-carbon. The barrier for the chelation of the methyl insertion is reasonably small; the barrier has a relative energy of −24.4 kcal mol^{-1}, an increase of only 4.8 kcal mol^{-1} from the intermediate. The same barrier for insertion into the amino bond reaches a relative energy of −1.3 kcal mol^{-1}, 25.3 kcal mol^{-1} above its intermediate. The amino intermediate must break the dative bonding interaction between the migrating dimethyl amino group and the aluminum center before the second nitrogen can chelate, which greatly increases this barrier. During the experimental insertion of carbodiimide into an aluminum amide bond, the presence of dangling imide moieties or exocyclic amide groups from other molecules could compensate for the energy needed to break the intramolecular Al−amide dative bond and lower this barrier. The steric effect of the *tert*-butyl ligand is largest here, as both barriers increase considerably over their values for diisopropyl carbodiimide insertion. For the methyl insertion, the relative energy of the chelation transition state for di-*tert*-butyl carbodiimide is 9.8 kcal mol^{-1} higher than that for diisopropyl carbodiimide. For the dimethyl amino insertion, the ^{t}Bu carbodiimide insertion is 13.3 kcal mol^{-1} higher than the same transition state of the diisopropyl insertion, reaching a relative energy of 12.0 kcal mol^{-1}.

Product. The net reaction energies show that the insertion into an Al−CH_3 bond is considerably more exergic than insertion into an Al−$N(CH_3)_2$ bond (−59.6 vs −36.1 kcal mol^{-1}, respectively, for diisopropyl carbodiimide insertion). This is predominantly the result of the relative bond strengths between the aluminum center and the migrating group. The G3MP2[14] calculated bond dissociation energies show that the H_2Al-CH_3 bond is weaker than the $H_2Al-N(CH_3)_2$ bond (119.6 and 136.3 kcal mol^{-1}, respectively). The amino group has a stronger ionic interaction with the aluminum center due to larger inductive effects, but it also can engage in π-type bonding between the lone-pair on the nitrogen and the empty p-orbital of the aluminum center.[15] Breaking this interaction causes the insertion into aluminum amino bonds to be less exergic than the insertion into a relatively weak aluminum methyl bond. The large exergicity of the alkyl insertion also shows that the deinsertion of the carbodiimide

(14) Curtiss, L. A.; Raghavachari, K.; Redfern, P. C.; Rassolov, V.; Pople, J. A. *J. Chem. Phys.* **1998**, *109*, 7764.
(15) Kormos, B. L.; Cramer, C. J. *Inorg. Chem.* **2003**, *42*, 6691.

from the acetamidinate product is much less likely than a deinsertion from the dimethyl amino insertion product.

Although insertion into these two bond types follows the same general reaction scheme, there are important differences in the reaction energetics, barrier heights, and geometries. For insertion of diisopropyl carbodiimide, the highest barrier for insertion into $Al-CH_3$ bonds is the migration transition state when the methyl group is migrating from the aluminum center to the sp-carbon. Conversely, for insertion into $Al-N(CH_3)_2$ bonds, the highest barrier occurs in the chelation transition state. Overall, the highest relative barrier for insertion into the $Al-CH_3$ bond is higher than the highest relative barrier for insertion into an $Al-N(CH_3)_2$ bond, which is consistent with the preferential insertion into aluminum amides reported by Chang et al.

For insertions into $Al-N(CH_3)_2$ bonds, the migration is facilitated by the lone-pair nitrogen of the dimethyl amino group, which reduces the migration barrier height. As there is no such stabilizing effect for the migration transition state for insertion into the $Al-CH_3$ bond, its transfer has a higher barrier. The relative energy of the chelation barrier is higher for insertion into the $Al-N(CH_3)_2$ bond than the $Al-CH_3$ bond; however, this barrier is still lower than the migration barrier height for insertion into the $Al-CH_3$ bond. The *tert*-butyl substituents on the carbodiimide have a particularly strong effect on the dimethyl amino insertion. Although the *tert*-butyl substitution also increases the barriers for the $Al-CH_3$ insertion, the $Al-CH_3$ insertion goes through its highest barrier in the migration transition state. The steric effect of the *tert*-butyl substituent is relatively small at this point because the migrating ligand is not yet in a close configuration with the R′ group. The $H_2Al-N(CH_3)_2$ insertion goes through its highest barrier in the chelation step, where the migrating ligand is in close proximity to the R′ group, so the steric repulsion between these two groups is the largest. Furthermore, the dimethyl amino group is larger than the methyl group, so it has a larger degree of steric repulsion with the *tert*-butyl group. This repulsion increases the chelation barrier of the dimethyl amino insertion above the migration barrier for the relative energy of the methyl insertion (9.3 vs 12.0 kcal mol^{-1}), implying the insertion into $Al-CH_3$ bonds is preferred to insertion into $Al-N(CH_3)_2$ for di-*tert*-butyl-carbodiimide, reversed from the order for diisopropyl carbodiimide.

Higher Order Insertions for Trimethylaluminum. Our first synthetic attempts to make five- and six-coordinate acetamidinates at room temperature were unsuccessful; when 3 equiv of diisopropyl carbodiimide was mixed with 1 equiv of trimethylaluminum at room temperature, the products after 1 week were aluminum monoacetamidinatodimethylaluminum and free carbodiimide, indicating (via NMR) that the second insertion effectively does not occur at room temperature. When 3 equiv of diisopropyl carbodiimide were refluxed with 1 equiv of trimethylaluminum at 100 °C for 48 h, trisacetamidinatoaluminum (**2**) was synthesized in good yield. Similarly, when 2 equiv of carbodiimide were refluxed with 1 equiv of trimethylaluminum, bisacetamidinatomonomethylaluminum (**1**) could be isolated, although it was

Scheme 4

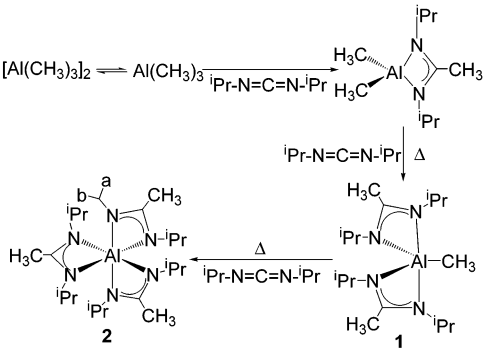

present in solution in proportions roughly equal to monoacetamidinate and trisacetamidinate. There appears to be a thermodynamic equilibrium of these insertion products, and this is a topic of ongoing research in our laboratory. No significant amount of **1** or **2** was synthesized until the temperature was raised above 70 °C (the reactions were refluxed for 24 h, and then the product ratios were observed via NMR). No reaction was observed when we attempted to insert diisopropyl carbodiimide directly into **1** at room temperature, indicating that the third insertion is also not observed at room temperature. These reactions are summarized in Scheme 4.

The proton NMR spectra of these two products are consistent with their proposed structures and demonstrate the difference in the steric environments of their ligands. In the case of **1**, only one spectroscopically distinguishable doublet representing the isopropyl methyl groups is found, as well as one septet for the isopropyl methine proton. This is caused by fluctuation of the solution structure to allow equilibration of the axial and equatorial nitrogen positions. In the case of **2**, there are two doublets of equal integration resolved for the isopropyl methyls (labeled "a" and "b" in Scheme 4), but only one septet can be seen from the methine group. This is consistent with a static chiral octahedral structure with two diastereotopic methyl groups.

The single-crystal X-ray diffraction was collected for compound **1**, and these data are summarized in Figure 3 and Tables 2−4.

Compound **1** possesses a strict C2 axis of symmetry and can be treated as having a metal center in a pseudo-trigonal bipyramidal coordination geometry. This compound possesses three equatorial groups (C1, N4, and N4b) that are coplanar with the sum of angles between these groups equal to 360°. The angle between the pseudoaxial positions shows a small distortion (159.63°) that we attribute to the limited bite angle of the amidinato ligands. As expected, the equatorial Al−N bonds (1.925 Å) were shorter than the axial distances (2.096 Å).

The nitrogen centers in the amidinate chelate ring show deviations from planarity. The sum of angles values around N2 and N4 are 357° and 359°, respectively. This can be attributed to steric congestion at the metal centers; this phenomenon has been seen in several group 13 amidinates and guanidinates.[3,5,16] As expected, the cyclic carbon has a planar sp^2 geometry, with a sum of angles of 360°.

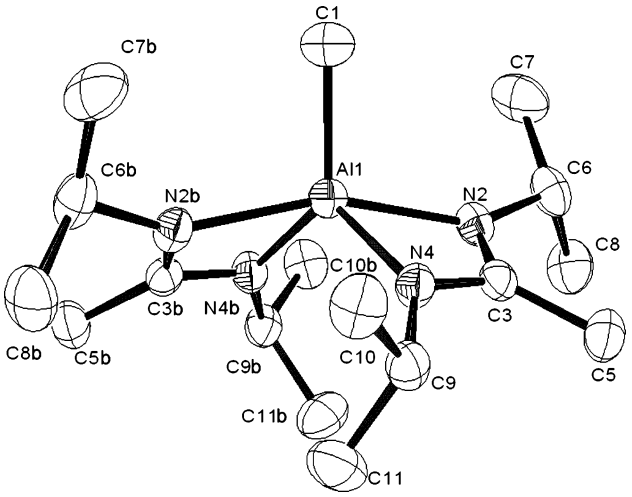

Figure 3. Molecular structure and atom numbering scheme for compound **1**. Hydrogen atoms have been omitted in every case for clarity, and thermal ellipsoids are shown at 50% probability.

Table 2. Crystal Data and Structure Refinement for $[CH_3C(N^iPr)_2]_2AlCH_3$ (**1**)

empirical formula	$C_{17}H_{37}AN_4$
formula weight	324.49
T (K)	209(2)
λ (Å)	0.71073
crystal system	monoclinic
space group	$C2/c$
unit cell dimensions	$a = 11.7644(14)$ Å
	$b = 12.8376(15)$ Å, $\beta = 107.644(2)°$
	$c = 14.1056(17)$ Å
V, Z	2030.1(4) Å^3, 4
P (calculated)	1.062 Mg/m^3
absorption coefficient	0.104 mm^{-1}
refinement method	full-matrix least-squares on F^2
R indices $[I > 2\sigma(I)]^a$	R1 = 0.0464, wR2 = 0.1074

^{a} $R1 = \sum||F_o| - |F_c||/\sum|F_o|$; $wR2 = (\sum w(|F_o| - |F_c|)^2/\sum w|F_o|^2)^{1/2}$.

Table 3. Selected Bond Lengths [Å] for $[CH_3C(N^iPr)_2]_2AlCH_3$ (**1**)

Al1−C1	1.969(2)
C3−N2	1.3215(19)
C3−N4	1.3388(18)
C3−C5	1.509(2)
Al1−N2	2.0960(12)
Al1−N4	1.9254(12)

Table 4. Selected Angles [deg] for $[CH_3C(N^iPr)_2]_2AlCH_3$ (**1**)

N4−Al1−N4b	114.69(8)
N4−Al1−C1	122.66
N2−Al1−N2b	159.62(7)
N4−Al1−N2	102.45(5)
∑ angles	
N2	357.2
N4	358.7
C3	360.0
torsion angles	
Al1−N2−C3−N4	0.3
C6−N2−C5−N4	166.5
C9−N4−C3−N2	169.0

On the basis of these experiments, we suspected that the second and third insertions have higher barrier heights than the first. To confirm this hypothesis, we calculated the reaction energies and barrier heights for the first and second insertion of diisopropyl carbodiimide into trimethylalumi-

Table 5. Calculated Barrier Heights and Reaction Energies for the First and Second Insertion of Carbodiimide into TMA^a

insertion	reactant state	separated	adduct	TS1	intermediate	TS2	product
first	monomer	0.0	−17.5	1.1	−26.6	−22.1	−54.2
	dimer	10.0	−7.4	11.2	−16.6	−12.0	−44.2
second	monomer	0.0	3.8	25.2	−26.1	−20.8	−35.7

^{a} The value for the dissociation of TMA is calculated by the G3MP2 method. All other values are calculated using BH&HLYP/6-311g(2d,2p)//BH&HLYP/6-31g(d). All values are in kcal mol^{-1}.

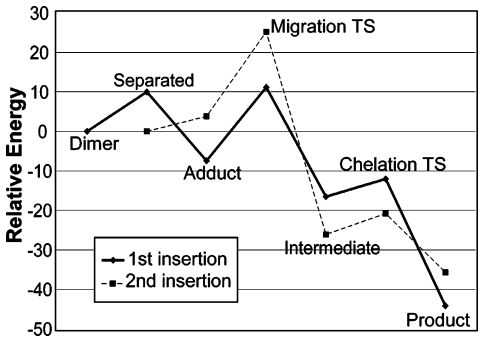

Figure 4. BH&HLYP/6-311g(2d,2p)/BH&HLYP/6-31g(d) gas-phase energy profile for the first and second insertion of diisopropyl carbodiimide into TMA. The energy of dissociation of the TMA dimer is calculated using G3MP2. Values are in kcal mol^{-1}.

num. Although the third insertion is too large to investigate given our current computational resources, the explanation as to why the third insertion is not possible at room temperature is likely to be analogous to the explanation of why the second insertion is not possible at room temperature.

First Insertion. Reexamining the first insertion using TMA instead of H_2Al-CH_3 showed an interesting trend. The energetic results are summarized in Table 5. The reaction profiles are plotted in Figure 4, and schematics of the stationary points and key bond lengths are reported in Figure 5.

The TMA adduct is less stable than the previously shown H_2Al-CH_3 adduct as there is greater steric repulsion between the carbodiimide and the methyl ligands of the aluminum center than for the hydride ligands. Furthermore, the additional electron-donating effects of the methyl groups decrease the electrophilicity of the aluminum center. The first transition state for insertion into TMA is actually more stable than the first transition state into H_2Al-CH_3 by 3.8 kcal mol^{-1}. In the TMA insertion, the migrating methyl group is moved away from the two other methyl groups on the aluminum center, decreasing steric repulsion between them and making the transition state more stable relative to the reactants. The product for the insertion into TMA is 5.4 kcal mol^{-1} more stable than the product for H_2Al-CH_3. The remaining points on the reaction coordinates are largely consistent with the analogous insertion into H_2Al-CH_3.

Second Insertion. One notable difference in the second insertion reaction coordinate is that the formation of the adduct in the second insertion is endergic by 3.8 kcal mol^{-1}. Natural population analysis (NPA)[17] shows that, although there is a roughly equal amount of electron donation from the inserting carbodiimide (the carbodiimide in the first

(16) Zhou, Y.; Richeson, D. S. *Inorg. Chem.* **1996**, *35*, 2448.

(17) Foster, J. P.; Weinhold, F. *J. Am. Chem. Soc.* **1980**, *102*, 7211.

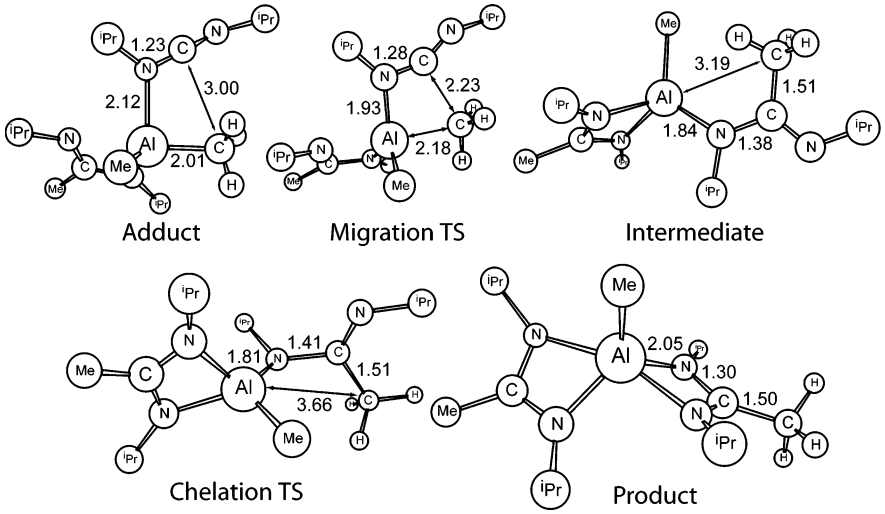

Figure 5. Schematic diagrams of the stationary points of the second insertion of diisopropyl carbodiimide into TMA. Key bond lengths (Å) are reported adjacent to the bonds.

adduct carries a charge of 0.137 as opposed to a charge of 0.132 in the second), the charge on the aluminum center effectively does not change when the carbodiimide coordinates to the monoacetamidinate (1.801 to 1.798). This can be rationalized by noting that in the optimized structure for the second insertion's adduct, the aluminum center has adopted a distorted trigonal planar form. This change in coordination involves the bond between one of the chelating nitrogens and the aluminum center increasing to a dative bond length (the calculated Al−N bond length is 2.3 Å). The N−C(sp^2) bonds in the acetamidinate ligand become asymmetrical, with one at a single bond length and the other at a double bond length. This rearrangement keeps the charge on the aluminum center roughly constant and eliminates the energetic benefit of the dative bonding interaction between the aluminum center and the carbodiimide, so the coordination of the carbodiimide does not facilitate the second insertion in the same way it did for the first insertion.

The most substantial difference between the first insertion and the second insertion is the migration barrier heights. This is due to the carbodiimide−TMA adduct that is formed in the initial step by an exergic reaction of dimerized TMA and carbodiimide. The adduct stage in the first insertion has a relative energy of −7.4 kcal mol^{-1}, which has the effect of lowering the migration barrier for this step, thereby allowing for a more facile migration of the methyl group. Because adduct formation in the second insertion is not exergic, its migration is not aided by the coordination of the carbodiimide. This effect can be observed in the geometry of the migration transition state for the second insertion. The Al−CH_3 bond is stretched to 2.65 Å at the migration transition state of the first insertion, while in the second insertion it is only stretched to 2.18 Å, indicating that the transition state occurs much earlier on the reaction coordinate for the second insertion. This can be rationalized by considering that the exergic adduct formation in the first insertion stabilizes the portion of the migration reaction coordinate where the structures are similar to the adduct, allowing the transition state structure to reflect a more stable intermediate-like structure. The second insertion's transition state more closely resembles the relatively unstable adduct.

This effect can also be seen in the NPA charge. For both the first and the second insertions, the net NPA charge on the carbodiimide switches from being positive in the adduct (0.137 for the first insertion, 0.132 for the second), due to the carbodiimide's behavior as a Lewis base, to being negative in the intermediate (−0.670 for the first insertion, −0.698 for the second), due to the carbodiimide's new role as an electron-withdrawing monodentate ligand. In the migration transition state of the first insertion, the charge distribution has already become similar to that of the intermediate, with the carbodiimide carrying a charge of −0.560. In the migration transition state of the second insertion, the carbodiimide has a net charge of −0.086, which more closely resembles the adduct's charge distribution. These geometrical and charge effects reflect a much higher relative energy for migration barrier for the first insertion than the second (11.2 vs 25.2 kcal mol^{-1}, respectively). The calculated barrier height for the second insertion is higher than we would expect to occur on the synthetic time scale even under reflux conditions. We suspect the BH&HLYP functional may have overestimated this barrier, although the qualitative trend remains consistent with the experimental observation that the second insertion does not proceed until the reaction temperature is increased above 70 °C.

The intermediate for the second insertion is actually more stable than the intermediate of the first insertion even when dimerization is taken into account. The second insertion's intermediate adopts a distorted tetrahedral geometry similar to the monoacetamidinate product, with the partially inserted amidinate ligand acting as a bulky dialkyl amino ligand. This intermediate is quite stable relative to the reactants and is only 9.6 kcal mol^{-1} less stable than the final product. This is the result of the general trend of four-coordinate monoacetamidinates being more stable than five-coordinate bisacetamidinates, as well as the high strength of Al−N bonds.

In each case, the chelation barrier after intermediate formation is small and has a much lower relative energy than

the migration barrier. The net reaction energy for the second insertion is −35.7 kcal mol^{-1}, as compared to −44.2 kcal mol^{-1} for the first insertion. The bite angle imposed on the ligand by the five-coordinate geometry is slightly smaller than in the four-coordinate form (67.4° vs 65.6°); however, a more substantial effect seems to be the larger degree of electron withdrawal from the aluminum center. This can be seen in the NPA charge on the aluminum center; after the first insertion, the aluminum center is approximately equally cationic as TMA monomer (1.792 vs 1.806). After the second insertion, the NPA charge has increased to 1.880, a significantly larger increase. Also, there is the effect of steric repulsion between the opposing isopropyl groups on the two acetamidinate rings; the shortest carbon to carbon distance between two methyl groups on opposite acetamidinate ligands is 3.87 Å. These effects can also be seen in the longer Al−N bond lengths in the products of each insertion; the bisacetamidinate Al−N bonds are 2.05 Å, an increase of 0.09 Å over the monoacetamidinate product.

Conclusions

We have defined a mechanism for the insertion of carbodiimide into three- and four-coordinate aluminum compounds and calculated the reaction energies and barrier heights for the insertion of diisopropyl and di-*tert*-butyl carbodiimides into both aluminum dimethyl amido bonds and aluminum methyl bonds.

We have found that a methyl group has a much higher barrier than a dimethyl amino group and that this barrier causes the insertion into Al−N(CH$_3$)$_2$ to be preferred over insertion into Al−CH$_3$ for diisopropyl carbodiimide because insertion into Al−CH$_3$ requires the methyl carbon to form a pentavalent transition state. The ability of the amide group to form a tetrahedral geometry through donation of its lone-pair during carbodiimide insertion into an Al−NMe$_2$ bond greatly reduces its barrier to insertion.

As well, the steric repulsion between the migrating group and the alkyl group of the carbodiimide causes the barrier height of the second step in the reaction to dominate for di-*tert*-butyl carbodiimide insertions, causing insertion into Al−CH$_3$ bonds to be preferred over insertion into Al−N(CH$_3$)$_2$ bonds. These results are consistent with the insertion preference reported in the literature.[5]

We have also extended this mechanism to the second insertion of diisopropyl carbodiimide into trimethylaluminum. Experimentally, only the first insertion occurs at room temperature, and the second and third insertions do not proceed at a significant rate until the reaction temperature is raised above 70 °C. This is consistent with our theoretical calculations that show that the second insertion into TMA goes through a 25.2 kcal mol^{-1} barrier, as compared to an effective barrier (including the dimerization of TMA) of 11.2 kcal mol^{-1} for the first insertion. As was proposed in the literature, the coordination of the carbodiimide to the metal center prior to the migration of the ligand is an important step in the insertions into three-coordinate aluminum species.[8,9] In the second insertion, the coordination is not exergic and therefore does not aid the reaction. As a result, this insertion goes through a considerably higher barrier.

Synthetically, we have reported the products for the second and third insertion of diisopropyl carbodiimide into trimethylaluminum, producing bisacetamidinatomonomethylaluminum (**1**) and trisacetamidinatoaluminum (**2**).

Experimental Section

General Procedures. All operations were carried out in a nitrogen filled drybox. The trimethyl aluminum and 1,3-diisopropyl carbodiimide were purchased from Aldrich and used as received. The hexane used was anhydrous grade, also purchased from Aldrich and used as received. The ^{1}H and ^{13}C NMR spectra were collected on a Bruker 400 MHz spectrometer using the residual protons in the deuterated solvent for reference. The deuterated benzene was purchased from Aldrich and used as received. Mass spectra were obtained using either the electron impact or the chemical impact method on a VG ZAB-2HF triple-focusing spectrometer.

[CH$_3$C(N^{i}Pr)$_2$]$_2$AlCH$_3$ (1). In a 150 mL pressure vessel, 4.0 mL of (CH$_3$)$_3$Al (2 M in hexane, 8.0 mmol) was added dropwise to 2 g of 1,3-diisopropyl carbodiimide (1.21 M in hexane, 12.0 mmol) while stirring rapidly over 30 min. The solution remained colorless. The reaction mixture was heated in an oil bath at 100 °C with the pressure vessel submerged to the level of the solution. It was heated while stirring for 24 h. The solution acquired a faint yellow color. The volatiles were removed under vacuum, leaving a discolored white powder. This powder was dissolved in hexane and recrystallized at −30 °C. After purification, compound **1** was collected as colorless needles (0.32 g, 12%). mp 81 °C. ^{1}H NMR (400 MHz, C$_6$D$_6$): 3.46 (sept, 4H, CH(Me)$_2$), 1.51 (s, 6H, (^{i}PrN)$_2$CMe), 1.23 (d, 24H, CH(CH$_3$)$_2$), −0.176 (s, 3H, AlCH$_3$). ^{13}C NMR (C$_6$D$_6$): 170.7 (NC(Me)N), 45.7 (CHMe$_2$), 24.7 (CHMe$_2$), 11.2 (^{i}PrN)CMe. Mass spectrum (EI, *m*/*z*) (rel intensity, %) 323 (0.2, [M − 1]$^+$), 309 (100.0, [M − CH$_3$]$^+$), 226 (0.8, [M − CH$_3$CN^{i}Pr − CH$_3$]$^+$), 183 (5.0, [M − CH$_3$C(N^{i}Pr)$_2$]$^+$), 169 (5.6, [(^{i}PrN)$_2$C(CH$_3$)Al)]$^+$), 142 (41.7, [^{i}PrNC(CH$_3$)N^{i}Pr + H]$^+$), 127 (9.6, [^{i}PrNCN^{i}Pr + 1]$^+$), 99 (4.2, [^{i}PrNCN^{i}Pr − CH$_3$]+), 84 (16.7, [^{i}PrNCN + 1]$^+$), 70 (13.9, ^{i}PrNC + 1]$^+$), 70 (65.9, [^{i}PrN]$^+$), 58 (55.8, [^{i}PrN+1]$^+$), 42 (81.4, [^{i}Pr − 1]$^+$). Anal. Calcd for AlC$_{17}$H$_{37}$N$_4$: C, 62.93; H, 11.49; N, 17.27. Found: C, 62.61; H, 11.07; N, 16.93.

[CH$_3$C(N^{i}Pr)$_2$]$_3$Al (2). In a 150 mL pressure vessel, 4.0 mL of (CH$_3$)$_3$Al (2 M in hexane, 8.0 mmol) was added dropwise to 3 g of 1,3-diisopropyl carbodiimide (1.48 M in hexane, 24.0 mmol) while stirring rapidly over 30 min. The solution remained colorless. The reaction mixture was heated in an oil bath at 100 °C with the pressure vessel submerged to the level of the solution. It was heated while stirring for 48 h. The solution had a faint yellow color. The volatiles were removed under vacuum, leaving a discolored white powder. This powder was dissolved in hexane and recrystallized at −30 °C. Compound **2** was collected as a white, amorphous powder (2.34 g, 65%). mp >320 °C. ^{1}H NMR (400 MHz, C$_6$D$_6$): 3.53 (sept, 2H, C*H*(Me)$_2$), 1.60 (s, 3H, (^{i}PrN)$_2$C*Me*), 1.32 (d, 6H, CH(C*H*$_3$)$_2$). 1.17 (d, 6H, CH(C*H*$_3$). ^{13}C NMR (C$_6$D$_6$): δ 168.3 (N*C*(Me)N), 46.5 (C*H*Me$_2$), 26.2 (CH*Me*$_2$), 24.1 (CH*Me*$_2$), 11.8 (*C*H$_3$C(N^{i}Pr)). Mass spectrum (CI, *m*/*z*) (rel intensity, %): 450 (17.8, M$^+$), 408 (0.6, [M − ^{i}Pr]$^+$), 366 (1.7, [M − ^{i}PrNC(CH$_3$)]$^+$), 323 (2.1, [M − ^{i}PrNCN^{i}Pr]$^+$), 309 (100, [M − ^{i}PrNC(CH$_3$)N^{i}Pr]$^+$), 295 (9.6, [M − ^{i}PrNC(CH$_3$)N^{i}Pr − CH$_3$]$^+$]$^+$), 267 (3.5, [M − ^{i}PrNC(CH$_3$)N^{i}Pr − ^{i}Pr]$^+$), 224 (11.8, [(CH$_3$C(N^{i}Pr)$_2$)AlN^{i}Pr]$^+$), 183 (18.3, [(CH$_3$C(N^{i}Pr)$_2$)AlCH$_3$]$^+$), 169 (23.1, [(CH$_3$C(N^{i}Pr)$_2$)Al]$^+$), 143 (28.3, [^{i}PrNC(CH$_3$)N^{i}Pr + 2]$^+$), 127 (11.7, [^{i}PrNCN^{i}Pr + 1]$^+$), 99 (6.4, [^{i}PrNC(CH$_3$)N] $^+$). Anal. Calcd for C$_{24}$H$_{51}$AlN$_6$: C, 63.96; H, 11.41; N, 18.65. Found: C, 63.55; H, 11.37; N, 19.00.

Structural Determinations for Compound 1. A single crystal was mounted on a thin glass fiber using viscous oil and then cooled to the data collection temperature. Crystal data and details of the measurements are included in the Supporting Information. Data were collected on a Bruker AX SMART 1k CCD diffractometer using 0.3° ω-scans at 0°, 90°, and 180° in ϕ. Unit-cell parameters were determined from 60 data frames collected at different sections of the Ewald sphere. Semiempirical absorption corrections based on equivalent reflections were applied. The structures were solved by direct methods, completed with difference Fourier syntheses, and refined with full-matrix least-squares procedures based on F^2. All non-hydrogen atoms were refined with anisotropic displacement parameters. All hydrogen atoms were treated as idealized contributions. All scattering factors and anomalous dispersion factors are contained in the SHELXTL 5.1 program library.

Computational Methods. All calculations were performed using the Gaussian-98 and Gaussian-03 packages of programs.[18,19] The method applied for calculation of reaction energies and barrier heights, denoted BH&HLYP/6-311g(2d,2p)//BH&HLYP/6-31g(d), uses the BH&HLYP functional[19−21] with a 6-31g(d) basis set to optimize the geometry of the molecules and to perform frequency calculations. This method was selected after extensive benchmarking studies that found that this method performed reasonably well at reproducing experimental bond dissociation enthalpies of aluminum compounds and in comparison to barrier heights found using the generally accurate CBS-Q method.[22,23] Details of these calculations are included in the Supporting Information. The (unscaled) frequencies were used for zero point correction to the electronic energy and to verify that the optimized structures are local minima. Following the optimization and frequency steps, electronic energies (E^{el}) were computed at the BH&HLYP/6-311g(2d,2p) level except where noted. All transition states were confirmed to have one imaginary frequency with the mode connecting the products and the reactants.

With respect to calculations including trimethylaluminum, it will dimerize via 3-center 2-electron bonds, so the inclusion of the energetics of this effect is important for comparing the relative barrier heights of the first and second insertions. Unfortunately, the DFT method used for the rest of the calculations gives a sizable error for the strength of the dimerization. Similar difficulties were reported with other common DFT functionals,[24] so this deficiency is not unique to the BH&HLYP functional. For this reason, the dimerization energies were also calculated using the G3MP2 method. The enthalpy of dissociation calculated using the G3MP2 method is 10.4 kcal mol^{-1}, which is in good agreement with the experimental value of 10.20 ± 0.17 kcal mol^{-1}.[25] As a result, we used the G3MP2 calculated energy of dissociation of 10.0 kcal mol^{-1} for our calculations of relative energies of reaction coordinates involving dimerized TMA. We believe this error is limited to the treatment of 3-center 2-electron bridging bonds and that the BH&HLYP functional is sufficiently accurate for calculations on the rest of systems under investigation based on the success of this functional in our benchmarking studies (see Supporting Information).

Acknowledgment. We acknowledge helpful suggestions by Erin Johnson, Owen Clarkin, Amanda Kenney, and Dr. Tom Woo. The 400 MHz NMR measurements were performed by Keith Borque, and mass spectral analysis was performed by Clem Kazakoff. Travel funds for C.N.R. were granted by the College of Natural Sciences, Carleton University.

Supporting Information Available: Benchmarking calculations, choice of methodology, Cartesian coordinates of all of the optimized structures, tables of atomic coordinates, isotropic displacement parameters, anisotropic displacement parameters, and bond distances and bond angles for **1**. This material is available free of charge via the Internet at http://pubs.acs.org.

IC048501Z

(18) Frisch, M. J.; Trucks, G. W.; Schlegel, H. B.; Scuseria, G. E.; Robb, M. A.; Cheeseman, J. R.; Zakrzewski, V. G.; Montgomery, J. A., Jr.; Stratmann, R. E.; Burant, J. C.; Dapprich, S.; Millam, J. M.; Daniels, A. D.; Kudin, K. N.; Strain, M. C.; Farkas, O.; Tomasi, J.; Barone, V.; Cossi, M.; Cammi, R.; Mennucci, B.; Pomelli, C.; Adamo, C.; Clifford, S.; Ochterski, J.; Petersson, G. A.; Ayala, P. Y.; Cui, Q.; Morokuma, K.; Salvador, P.; Dannenberg, J. J.; Malick, D. K.; Rabuck, K.; Raghavachari, J. B.; Foresman, J.; Cioslowski, J. V.; Ortiz, A. G.; Baboul, B. B.; Stefanov, A. D.; Liu, G.; Liashenko, A.; Piskorz, P.; Komaromi, I.; Gomperts, R.; Martin, R. L.; Fox, D. J.; Keith, T.; Al-Laham, M. A.; Peng, C. Y.; Nanayakkara, A.; Challacombe, M.; Gill, P. M. W.; Johnson, B.; Chen, W.; Wong, M. W.; Andres, J. L.; Gonzalez, C.; Head-Gordon, M.; Replogle, E. S.; Pople, J. A. *Gaussian 98*, revision A.9; Gaussian, Inc.: Pittsburgh, PA, 2001.

(19) Frisch, M. J.; Trucks, G. W.; Schlegel, H. B.; Scuseria, G. E.; Robb, M. A.; Cheeseman, J. R.; Montgomery, J. A., Jr.; Vreven, T.; Kudin, K. N.; Burant, J. C.; Millam, J. M.; Iyengar, S. S.; Tomasi, J.; Barone, V.; Mennucci, B.; Cossi, M.; Scalmani, G.; Rega, N.; Petersson, G. A.; Nakatsuji, H.; Hada, M.; Ehara, M.; Toyota, K.; Fukuda, R.; Hasegawa, J.; Ishida, M.; Nakajima, T.; Honda, Y.; Kitao, O.; Nakai, H.; Klene, M.; Li, X.; Knox, J. E.; Hratchian, H. P.; Cross, J. B.; Adamo, C.; Jaramillo, J.; Gomperts, R.; Stratmann, R. E.; Yazyev, O.; Austin, A. J.; Cammi, R.; Pomelli, C.; Ochterski, J. W.; Ayala, P. Y.; Morokuma, K.; Voth, G. A.; Salvador, P.; Dannenberg, J. J.; Zakrzewski, V. G.; Dapprich, S.; Daniels, A. D.; Strain, M. C.; Farkas, O.; Malick, D. K.; Rabuck, A. D.; Raghavachari, K.; Foresman, J. B.; Ortiz, J. V.; Cui, Q.; Baboul, A. G.; Clifford, S.; Cioslowski, J.; Stefanov, B. B.; Liu, G.; Liashenko, A.; Piskorz, P.; Komaromi, I.; Martin, R. L.; Fox, D. J.; Keith, T.; Al-Laham, M. A.; Peng, C. Y.; Nanayakkara, A.; Challacombe, M.; Gill, P. M. W.; Johnson, B.; Chen, W.; Wong, M. W.; Gonzalez, C.; Pople, J. A. *Gaussian 03*, revision C.02; Gaussian, Inc.: Pittsburgh, PA, 2003.

(20) Lee, C.; Yang, W.; Parr, R. G. *Phys. Rev. B: Condens. Matter* **1988**, *37*, 785.

(21) Becke, A. D. *J. Chem. Phys.* **1993**, *98*, 5648.

(22) Ochterski, J. W.; Petersson, G. A.; Montgomery, J. A., Jr. *J. Chem. Phys.* **1996**, *104*, 2598.

(23) Malick, D. K.; Petersson, G. A.; Montgomery, J. A., Jr. *J. Chem. Phys.* **1998**, *108*, 5704.

(24) Willis, B. G.; Jensen, K. F. *J. Phys. Chem. A* **1998**, *102*, 2613.

(25) Henrickson, C. H.; Duffy, D.; Eyman, D. P. *Inorg. Chem.* **1968**, *7*, 1047.